NASA TECHNICAL NOTE

NASA TN D-6377

NASA TN D-6377

EFFECT OF DIFFUSERS, SHROUDS, AND MASS INJECTION ON THE STARTING AND OPERATING CHARACTERISTICS OF A MACH 5 FREE JET TUNNEL

by John K. Molloy, Ernest A. Mackley, and J. Wayne Keyes

Langley Research Center
Hampton, Va. 23365

NATIONAL AERONAUTICS AND SPACE ADMINISTRATION • WASHINGTON, D. C. • SEPTEMBER 1971

1. Report No.	2. Government Accession No.	3. Recipient's Catalog No.
NASA TN D-6377		

4. Title and Subtitle	5. Report Date
EFFECT OF DIFFUSERS, SHROUDS, AND MASS INJECTION ON THE STARTING AND OPERATING CHARACTERISTICS OF A MACH 5 FREE-JET TUNNEL	September 1971
	6. Performing Organization Code
7. Author(s)	8. Performing Organization Report No.
John K. Molloy, Ernest A. Mackley, and J. Wayne Keyes	L-7659
	10. Work Unit No.
9. Performing Organization Name and Address	764-75-01
NASA Langley Research Center Hampton, Va. 23365	11. Contract or Grant No.
	13. Type of Report and Period Covered
12. Sponsoring Agency Name and Address	Technical Note
National Aeronautics and Space Administration Washington, D.C. 20546	14. Sponsoring Agency Code

15. Supplementary Notes

16. Abstract

An experimental investigation was conducted in a Mach 5 free-jet tunnel to assess the problem of establishing supersonic flow with a high blockage model and to devise a model-tunnel test-section configuration which would allow flow establishment ("tunnel starting") at low pressure ratios. The model had a cross-sectional area equal to approximately 50 percent of the nozzle exit area. Two tunnel diffuser sizes with some combinations of model shroud configurations, and Mach 4 annular injectors at the nozzle exit and the diffuser entrance were investigated. Starting pressure ratios on the order of 50 and ratios of chamber pressure to free-stream static pressure of 1.0 were obtained during these tests.

17. Key Words (Suggested by Author(s))	18. Distribution Statement
Starting characteristics Diffusers Shrouds Mass injection Free-jet tunnel	Unclassified – Unlimited

19. Security Classif. (of this report)	20. Security Classif. (of this page)	21. No. of Pages	22. Price*
Unclassified	Unclassified	30	$3.00

*For sale by the National Technical Information Service, Springfield, Virginia 22151

EFFECT OF DIFFUSERS, SHROUDS, AND MASS INJECTION ON THE STARTING AND OPERATING CHARACTERISTICS OF A MACH 5 FREE-JET TUNNEL

By John K. Molloy, Ernest A. Mackley,
and J. Wayne Keyes
Langley Research Center

SUMMARY

An experimental investigation was conducted in a Mach 5 free-jet tunnel to assess the problem of establishing supersonic flow with a high blockage model and to devise a model-tunnel test-section configuration which would allow flow establishment ("tunnel starting") at low pressure ratios. Various combinations of tunnel diffuser size, model shroud configurations, and annular Mach 4 injectors at the nozzle exit and the diffuser entrance were investigated. The investigation was conducted at the Langley Research Center in a test chamber, which was modified to provide a 1/10-scale model of the Lewis free-jet hypersonic propulsion research facility. A model which had a cross-sectional area that was approximately 50 percent of the nozzle exit area was used in this investigation. With the model in the test position, supersonic flow could not be achieved, even at extremely high ratios of tunnel stagnation to diffuser-exit static pressure. The addition of a model shroud, which was designed to provide an annular passage between the conical entrance to the tunnel diffuser and the external surface of the shroud, allowed supersonic flow to be established with a pressure ratio of 92 and a ratio of test-chamber pressure to free-stream pressure of 2.8 was attained. With a similar type of shroud configuration, except for the addition of a ring at the shroud entrance, which was designed to restrict any reverse flow, supersonic flow was established with a pressure ratio of 47 and a ratio of test-chamber pressure to free-stream static pressure of 1.9 was attained.

When Mach 4 annular injectors at the nozzle and the diffuser entrance were used in conjunction with this shroud configuration, the starting characteristics were slightly improved and a ratio of test-chamber pressure to free-stream static pressure of 1.0 was attained. The experimental results show, however, that for a shroud configuration which did not have an annular passage between the conical entrance to the tunnel diffuser and the external surface of the shroud, mass injection from the Mach 4 annular injector at the nozzle exit was required to establish supersonic flow. In addition, the lowest ratio of chamber pressure to nozzle static pressure attainable with this type of shroud configuration was 1.9.

INTRODUCTION

Testing of hypersonic airbreathing engines requires wind tunnels with heated, high-pressure air supplies; cost factors tend to reduce the tunnel size, but the experimenter generally wishes to conduct tests with a relatively large model. However, since models with large cross-sectional areas relative to the tunnel test-section area create starting problems (refs. 1 and 2), which are not amenable to an analytical solution, an experimental program was undertaken to develop simple expedients to achieve in-place starting with the characteristically high blockages associated with full-scale testing of airbreathing engines.

This paper presents the results of an experimental study conducted in a Langley test chamber to determine means to improve the starting and operational characteristics of a free-jet wind tunnel with high blockage. Tests at Mach 4, 5, and 7 were made in this study; however, only the Mach 5 results, which are similar to the results obtained at Mach 4 and 7, are presented in this paper. The test chamber was modified to provide a 1/10-scale model of the Lewis free-jet hypersonic propulsion research facility. The model was a 1/10-scale model of a hypersonic research engine and had a maximum cross-sectional area of approximately 50 percent of the nozzle exit area. This blockage was sufficiently large to raise questions as to the possibility of establishing supersonic flow with the model in place. The test arrangements which were used to achieve in-place starting included tunnel diffuser size, various model shroud configurations, and annular Mach 4 injectors at the tunnel nozzle exit and the diffuser entrance.

The model shrouds used in the present tests are larger in diameter at the front than at the tunnel nozzle exit; thereby, the entire tunnel stream is captured and ducted. In contrast, the "jet-stretcher" concept (refs. 3 and 4) utilizes a shroud which is smaller than the tunnel nozzle and protects the model from shock-wave reflections. With a jet stretcher, the longitudinal external pressure distribution on the model remains more like that for actual flight for a longer model length; the jet is thereby "stretched." Although the jet stretcher may, or may not, favorably affect the tunnel starting because of changes in the overall total-pressure loss, the prime purpose is aerodynamic and not like the present shroud configurations, a means of achieving easier tunnel starting.

The pressure ratios, stagnation pressure to the diffuser exit static pressure, necessary for tunnel starting are presented for the model-tunnel test-section configurations that allowed supersonic flow to be established. In addition, the ratios of the chamber static pressure to free-stream static pressure are presented as an indication of the operating performance of the various configurations.

SYMBOLS

A_1, A_2, A_3 annular areas between external surface of model shroud and inner surface of tunnel diffuser

D diffuser diameter

d tunnel nozzle exit diameter

l free-jet length, distance from exit of tunnel nozzle or annular injector to leading edge of diffuser or model shroud

$\dot{m}$ mass flow rate

p static pressure

p_e static pressure at downstream end of diffuser constant-area section

p_t total pressure

$\left(p_{t,\infty}/p_e\right)_1$ overall pressure ratio, where p_e is determined after model injection

$\left(p_{t,\infty}/p_e\right)_2$ overall pressure ratio, where p_e is determined with model in place and with $p_{t,\infty} = 0$ (just prior to flow initiation)

$\left(p_{t,\infty}/p_e\right)_3$ overall pressure ratio, where p_e is determined with model in place and with $p_{t,\infty} = 0$ (just prior to flow initiation) and injector(s) operating at a stagnation pressure of 0.689 MN/m^2

$\left(p_{t,\infty}/p_e\right)_{restart}$ restart pressure ratio, where p_e is determined after supersonic flow is reestablished

R_d free-stream Reynolds number based on d

r_s shroud radius

x,r tunnel and model ordinates

y diffuser vertical height

α model angle of attack

ϕ angle in plane perpendicular to X-axis

Subscripts:

c chamber

j jet

∞ free stream

APPARATUS AND MODELS

A schematic of the apparatus and the hypersonic research engine (aerothermodynamic integration model) (HRE (AIM)) model is shown in figure 1. The air supply to the nozzle test chamber has a maximum pressure and temperature of 3.45 MN/m^2 and 534 K, respectively. The Mach 5 contoured nozzle that was used in this investigation has an exit diameter of 10.56 cm and was designed for a stagnation pressure of 3.45 MN/m^2. The tunnel flow exhausts from the test chamber through a diffuser and vacuum system to an 18.29-meter-diameter vacuum sphere. The point at which simulation of the hypersonic propulsion research facility (HPRF) terminates is noted in figure 1. In the HPRF the flow is to be spray cooled by water in the expanding section of the diffuser, and this section is to be followed by a constant area pipe which houses a center-fed steam ejector. The test chamber used in these tests at Langley is not equipped with a steam ejector; however, simulation of the starting pressure ratios available in the Lewis HPRF was accomplished through the use of the facility vacuum system. These tests simulate the stagnation pressure at which the HPRF will operate but do not simulate total temperature. The total temperature during this investigation was 378 K, whereas in the HPRF it will be 1222 K.

The pertinent dimensions of the 1/10-scale engine model and the location of the model static orifices are shown in figure 2. The model inlet spike position represents the closed no-through-flow position. An airflow-metering device (see fig. 2) will be attached to the full-scale engine in place of the engine nozzle plug so that the engine airflow rate can be determined. This device was also simulated in the present tests. To simulate full-scale testing at angle of attack, wedges were placed between the engine model and the mounting plate to give a model angle of attack of -4.5°.

Figure 3 shows the details of the two tunnel diffusers that were investigated. Diffuser A, which simulates the HPRF diffuser, has a constant area section which is

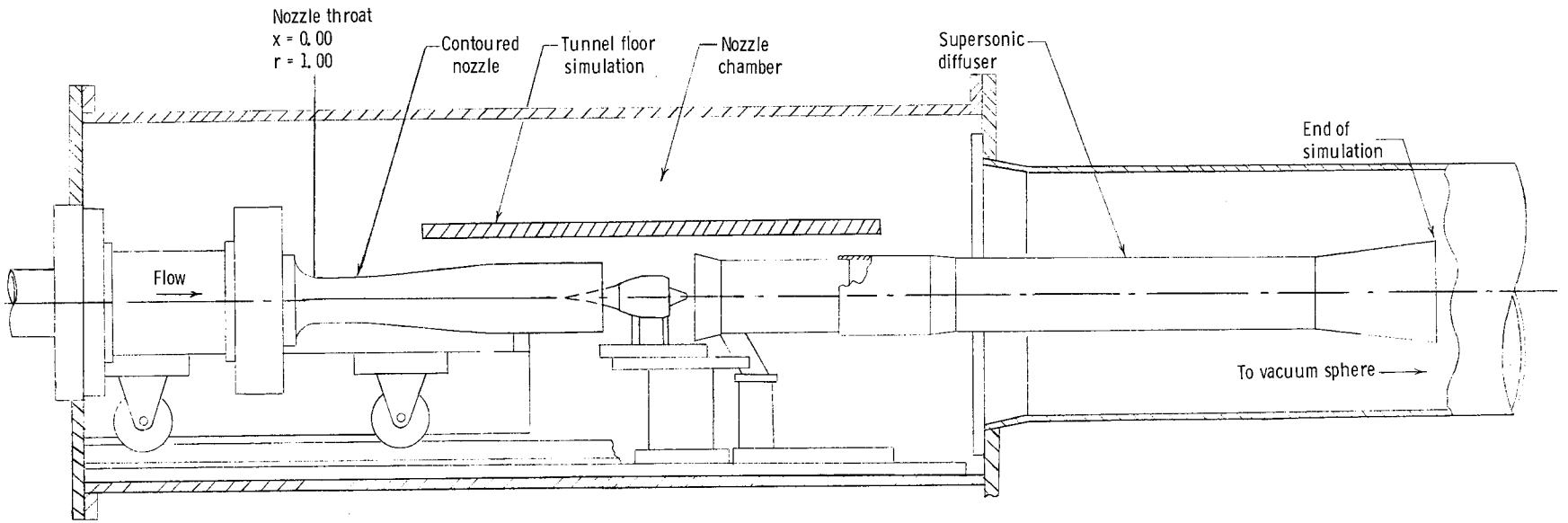

Figure 1.- Schematic of apparatus and hypersonic research engine (aerothermodynamic integration model).

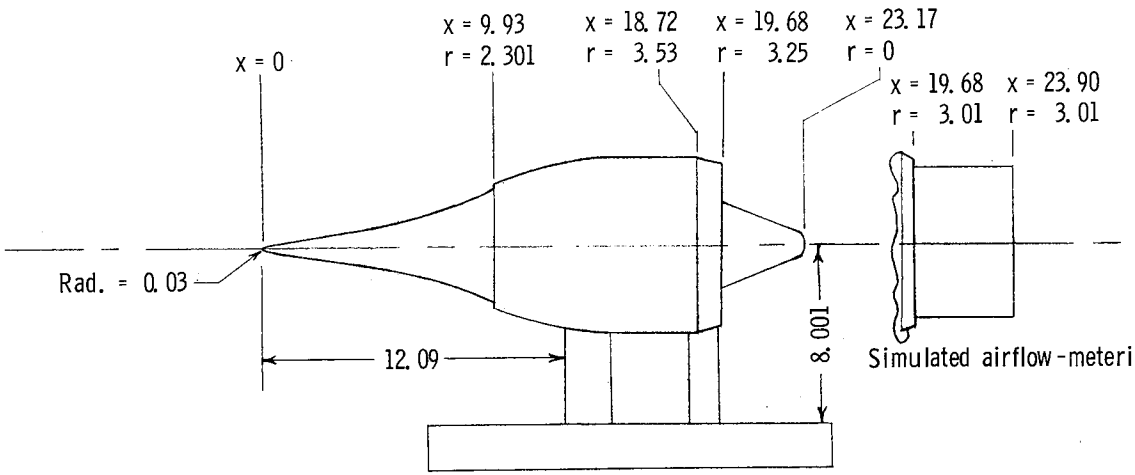

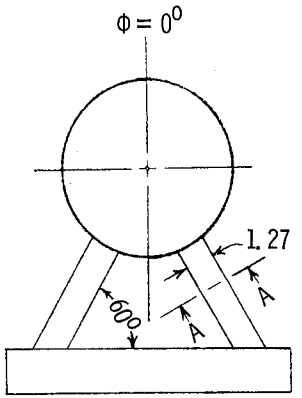

Orifice coordinate, x,
along Φ = 0°

5.08
7.37
10.16
12.70
16.51

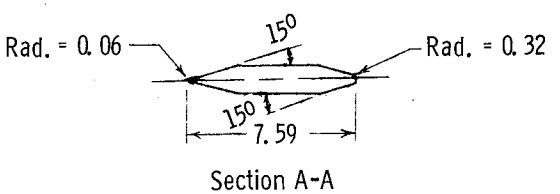

Section A-A

Figure 2.- Sketch of HRE (AIM) model. (All dimensions are in centimeters.)

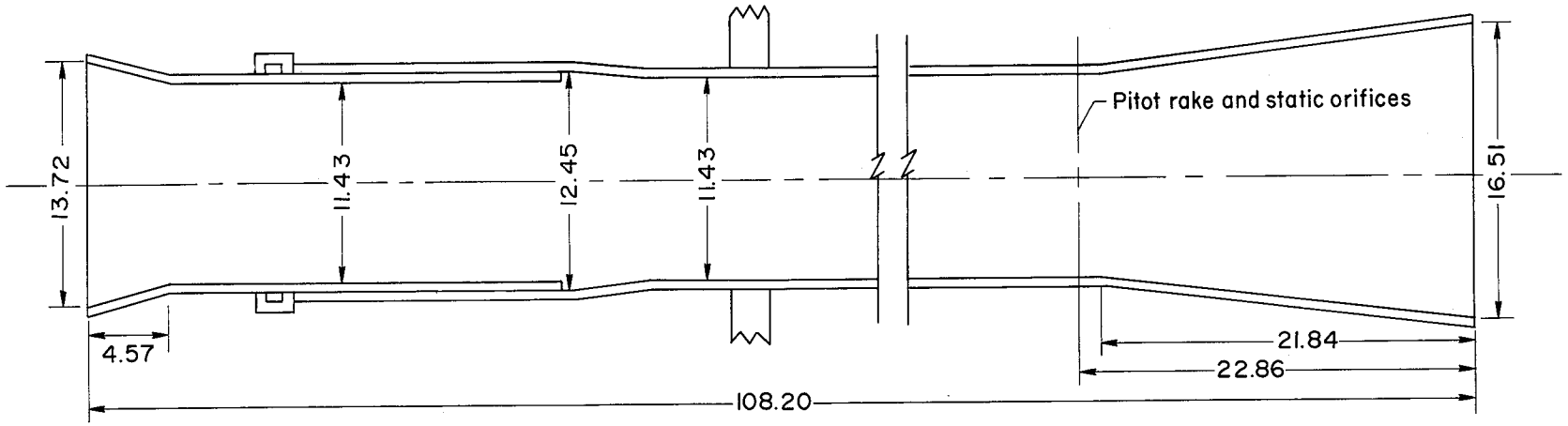

Diffuser A

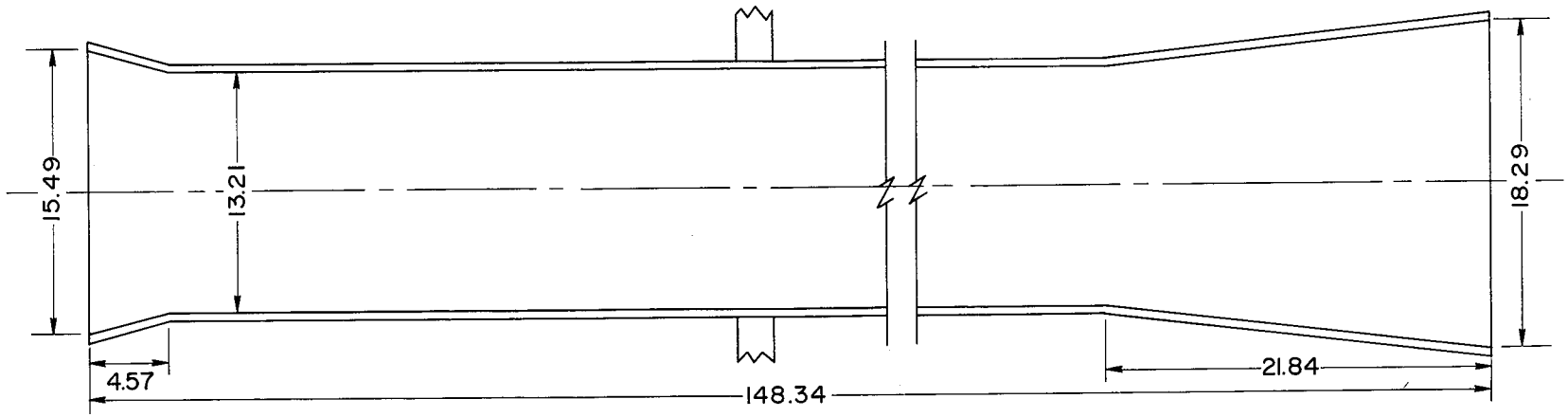

Diffuser B

Figure 3.- Diffuser configurations. (All dimensions in centimeters.)

17 percent greater than the nozzle exit area, and the ratio of length to the diameter at the constant area section is 9.5. Mach number and pressure recovery were determined near the end of the diffuser constant-area section of diffuser A. Diffuser B has a constant-area section which is 56 percent greater than the nozzle exit area and the ratio of length to the diameter of the constant-area section is 11.2.

The starting characteristics of four model-tunnel test-section configurations were investigated. A description of each follows.

Configuration I, Model Injection

Figure 4 illustrates configuration I, which is the test-section arrangement for injecting the model after supersonic flow has been established in the test section. Diffuser A was used for these tests; the ratio of free-jet length to nozzle diameter l/d required to inject the model from the side was 2.16.

Configuration II, Diffuser Diameter

Configuration II, which is a model test-section arrangement for starting the tunnel with the model in place, is shown in figure 5. In order to find the effect of diffuser diameter on the starting characteristics, both diffusers A and B were tested with this configuration. This was the only configuration of which diffuser B was a part. An extension to the forward conical section of diffuser A (see fig. 5) was investigated. The ratio of l/d for the basic diffuser configuration was 1.44 and the extension to diffuser A decreased the free-jet length from 1.44 to 1.22 nozzle exit diameters.

Configuration III, Shroud

A sketch of this configuration is shown in figure 6. The purpose of shrouding the model is to channel the tunnel flow around the model and to induce a flow through an annular area created between the external surface of the shroud, and the conical entrance to the tunnel diffuser, and thereby pump the test chamber down in pressure. This pumping action is similar to an ejector; in this case the primary flow is the wind-tunnel stream. After passing around the model, the tunnel stream expands to a pressure lower than the test-chamber pressure, and thereby provides the pressure difference between the chamber and the main stream which is necessary to provide the pumping action of the secondary flow. The annular area A_1 could be varied by moving the tunnel diffuser relative to the shroud. Two similar shroud configurations, shrouds 1 and 2, were investigated and their dimensions are given in figure 6. A free-jet length of 0.375 nozzle exit diameters was used with both shroud configurations. The difference in the shroud configurations is in the entrance and the exit areas. The area between the model mounting struts and the shroud was sealed in order to prevent any leakage of the high internal shroud pressure into the chamber.

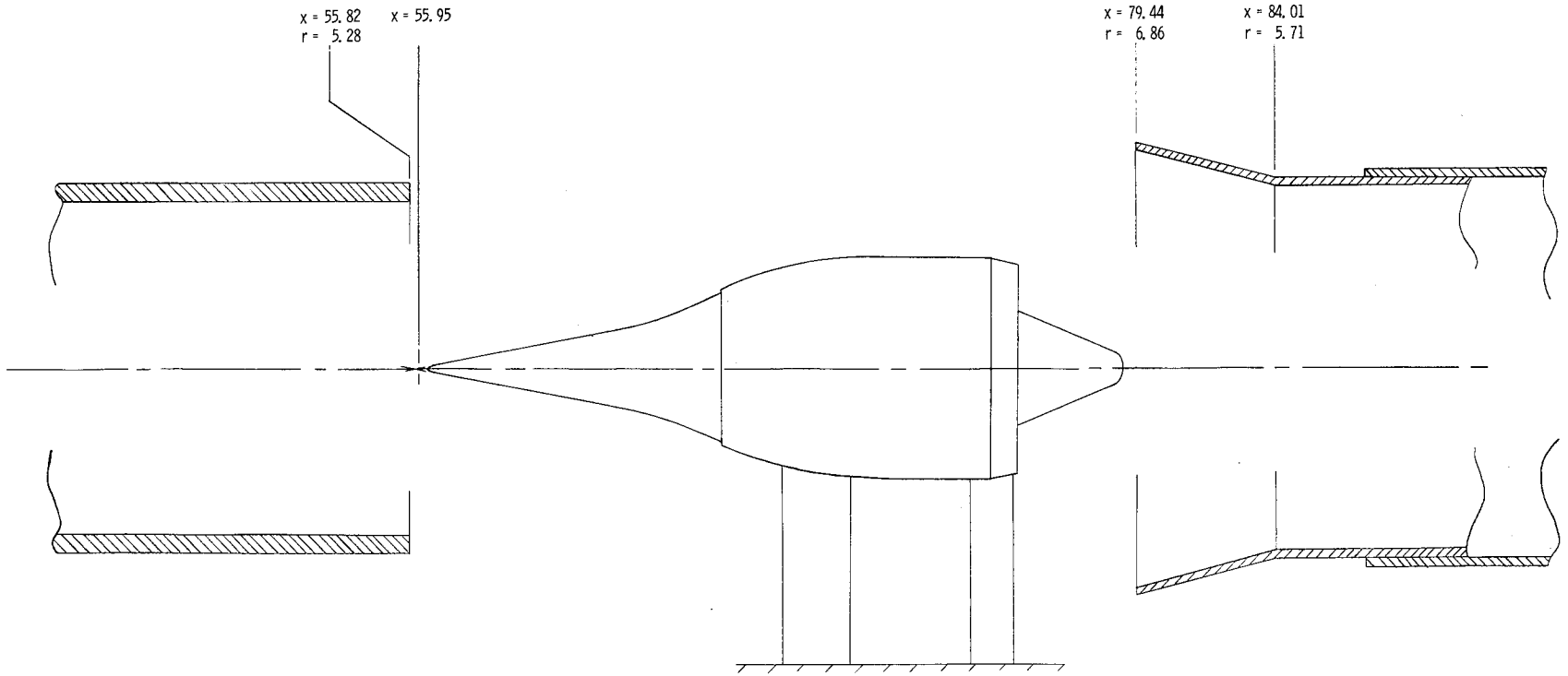

Figure 4.- Schematic of configuration I, $l/d = 2.16$; $x = 0.0$ at nozzle throat. (All dimensions are in centimeters.)

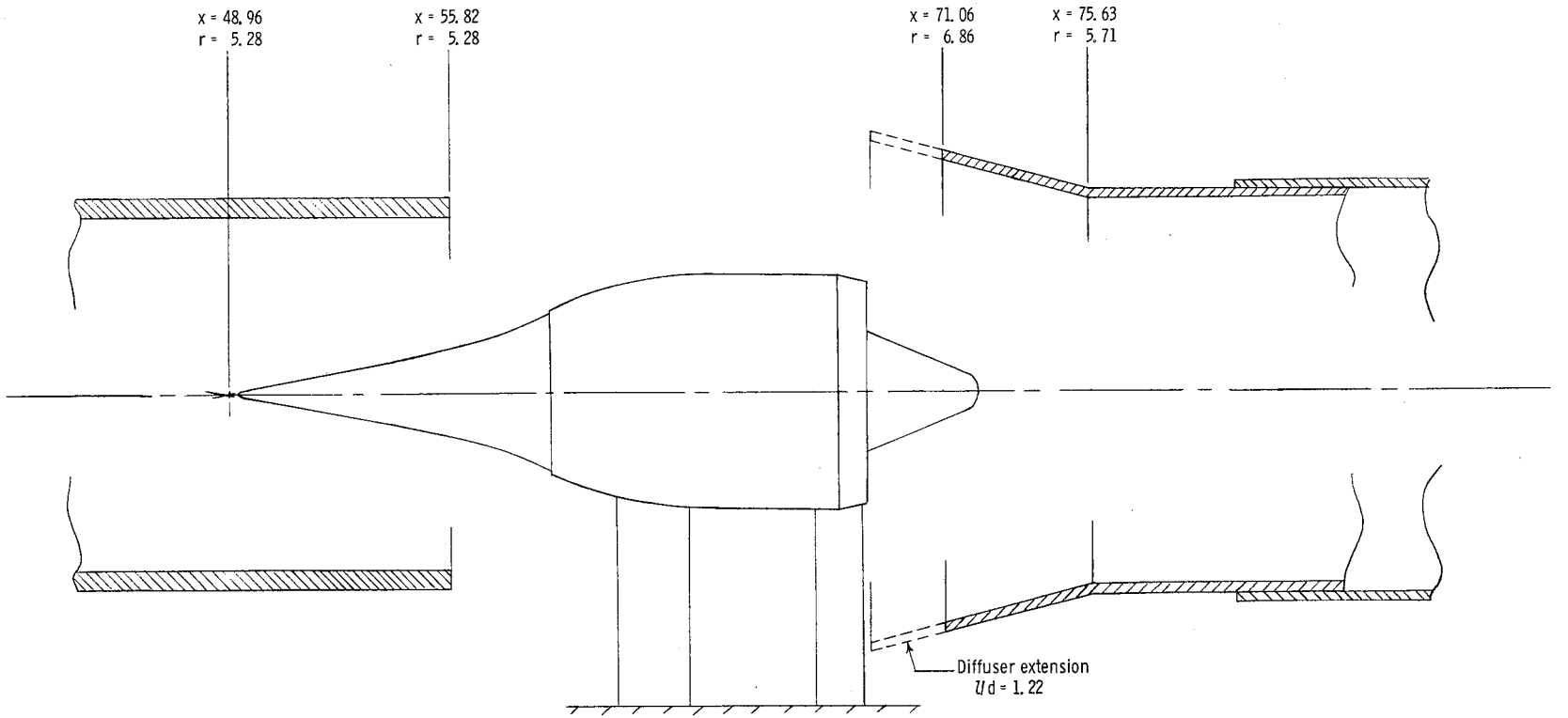

Figure 5.- Schematic of configuration II, $l/d = 1.44$; x = 0.0 at nozzle throat. (All dimensions are in centimeters.)

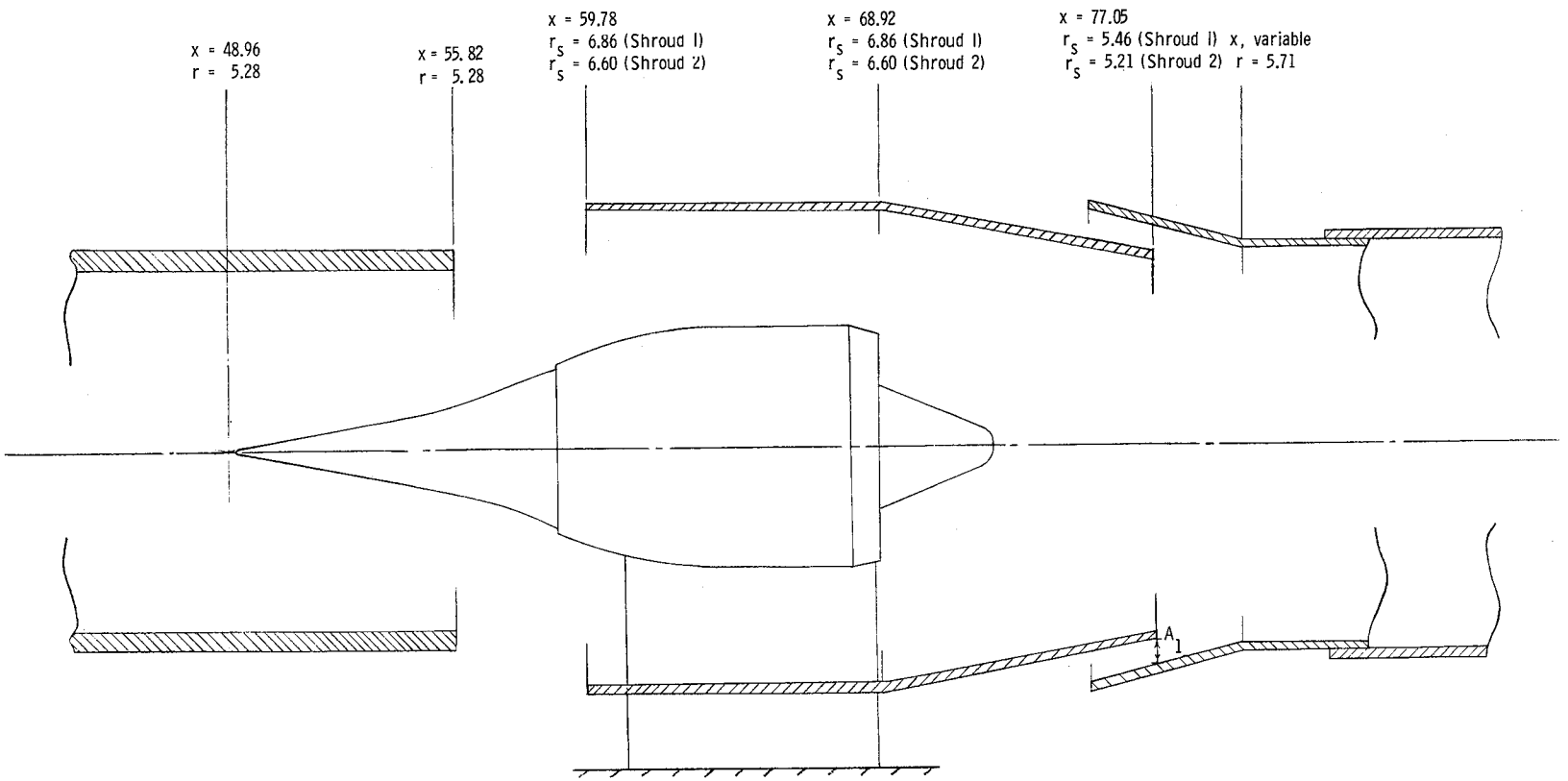

Figure 6.- Schematic of configuration III, shrouds 1 and 2. $l/d = 0.375$; x = 0.0 at nozzle throat. (All dimensions are in centimeters.)

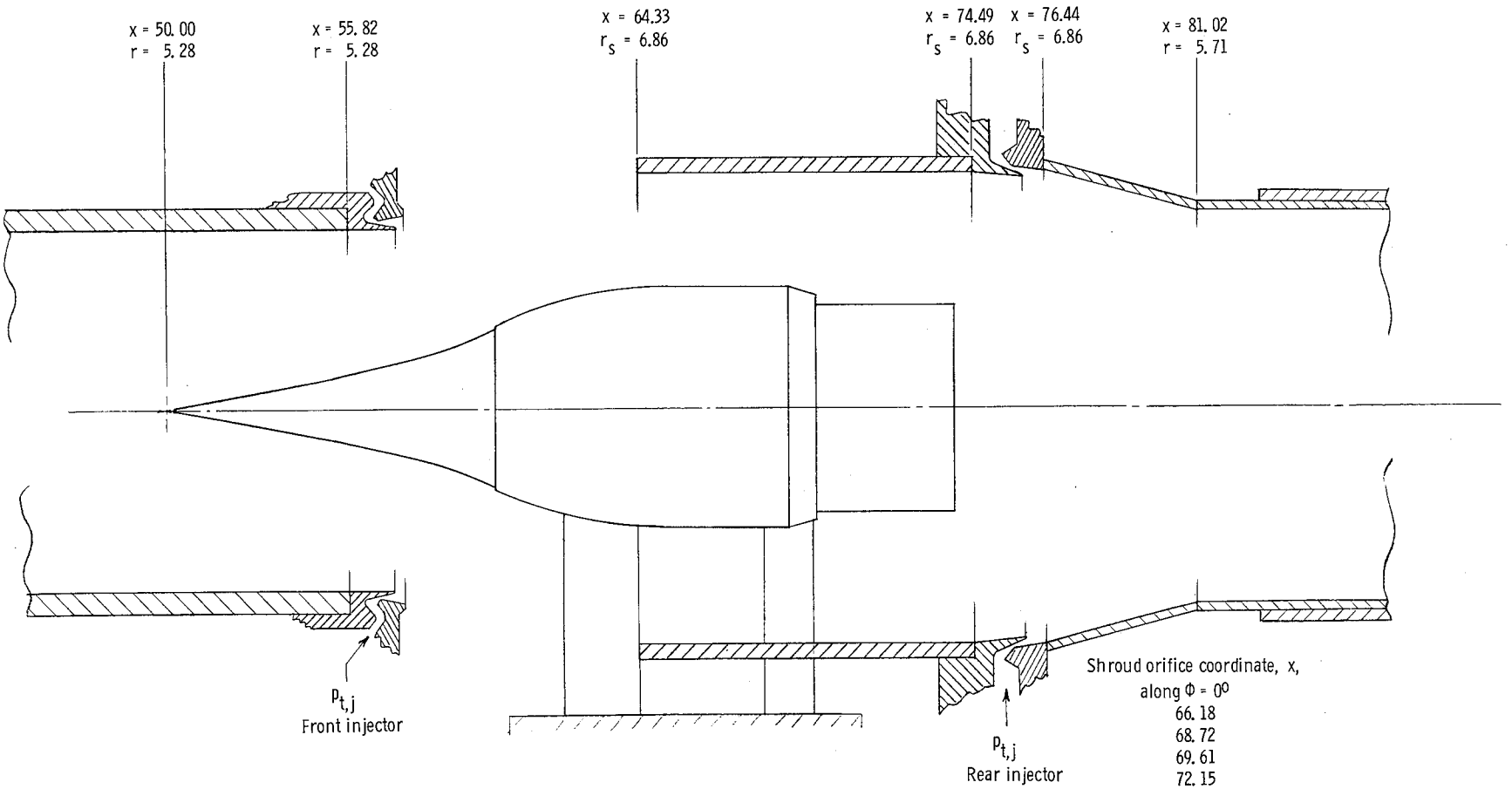

(a) Shroud 3; $l/d = 0.690$; x = 0.0 at nozzle throat.

Figure 7.- Schematic of configuration IV. (All dimensions are in centimeters.)

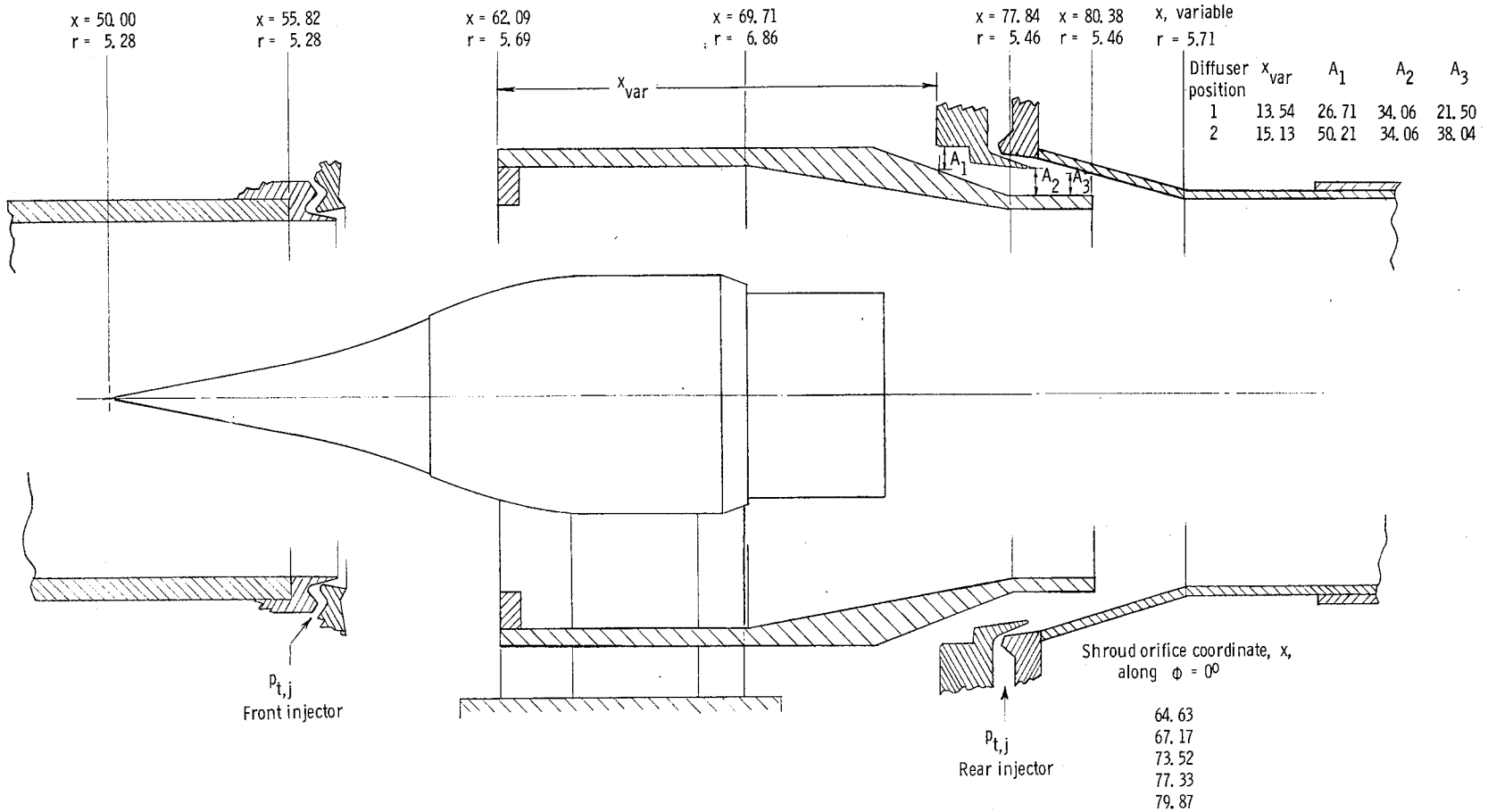

(b) Shroud 4; $l/d = 0.480$; x = 0.0 at nozzle throat.

Figure 7.- Concluded.

Configuration IV, Shrouds Plus Annular Injectors

Configuration IV consists of two different model shroud configurations, shrouds 3 and 4, in conjunction with Mach 4 annular injectors at the nozzle exit (front injector) and the diffuser entrance (rear injector). (See fig. 7.) The area between the model mounting struts and the shroud was sealed. The use of annular injectors to extend the operating range of wind tunnels has been previously reported in reference 5. Gas injection increases the level of the stream momentum in the tunnel nozzle boundary layer, inhibits boundary-layer separation, and thus reduces the necessary pressure ratio for establishing supersonic flow. The geometry of the annular injector nozzles used in this investigation are shown in figure 8. The average total temperature of the injected air was 289 K and the maximum stagnation pressure was 0.8 MN/m^2. The design throat areas for the front injector (attached to the nozzle) and the rear injector (attached to the diffuser) were 0.949 and 0.981 cm^2, respectively. Both annular injectors were operated from the same manifold. Shutoff valves in the lines from the manifold to the settling chamber of each injector enabled the front or rear injector to be operated separately. However, when both injectors were operated simultaneously, the stagnation pressure of one could not be varied independently of the other; and furthermore, because of a difference in the supply-line pressure loss, the stagnation pressure of one injector could not be matched to the other.

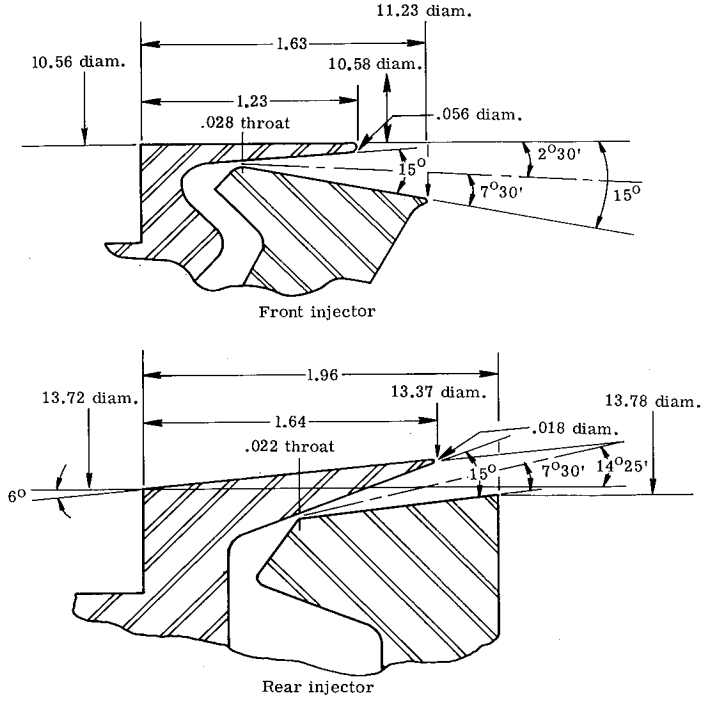

Figure 8.- Sketch of Mach 4 annular injector nozzles.
(All dimensions are in centimeters.)

Figure 9 shows the variation between the front and the rear injector stagnation pressure for simultaneous operation.

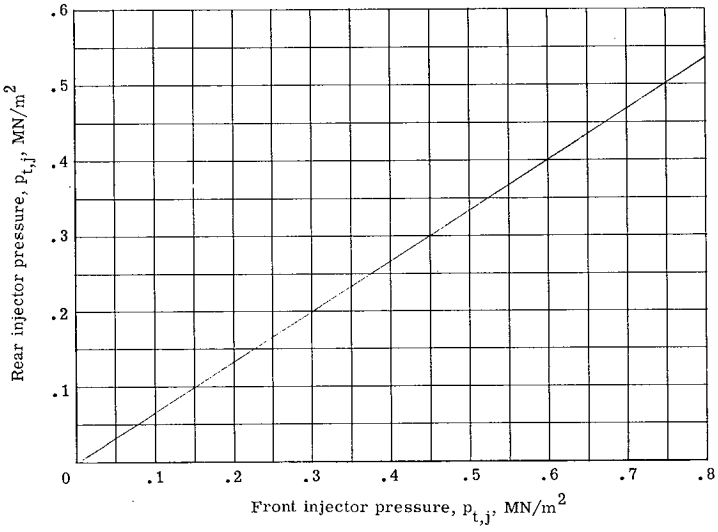

Figure 9.- Rear injector pressure as a function of front injector pressure.

Shroud 3 (fig. 7(a)) has a constant area and connects directly to the rear injector. The leading edge of the shroud coincides with the rear of the wedge leading-edge section of the model mounting struts. The distance from the end of the inner part of the front annular injector to the leading edge of the shroud was 0.69 nozzle exit diameters. Shroud 4 (fig. 7(b)) is similar to the shrouds used in configuration III, but has a ring at the entrance and a short constant-area section at the shroud exit. The distance from the end of the inner part of the front annular injector to the leading edge of the shroud was 0.480 nozzle exit diameters. By moving the diffuser relative to the shroud, the annular area between the shroud and the rear injector could be varied. The two positions that were investigated are designated in figure 7(b). The purpose of the ring at the front end of the shroud was to prevent any reverse flow along the inside of the shroud from spilling into the test chamber. Unreported test results of a similar shroud configuration at Mach 7 indicated that such a ring reduced the starting pressure ratio necessary to establish supersonic flow. The purpose of the short constant-area section at the shroud exit was to provide a good approach to the mixing point of the injector and tunnel flows.

In order to find the effect of angle of attack on the starting characteristics, the model was rotated about a point on the model center line which was 11.54 cm from the spike tip to an angle of attack of -4.5°. The model shroud was not rotated with the model.

TESTS AND ACCURACY

Establishment of supersonic flow in the test section was determined visually through the use of a schlieren system and by a visual display of the nozzle exit static pressure.

An overall pressure ratio is used in this report to define the tunnel starting and operational characteristics. Because of differences in the testing procedures, the definition of overall pressure ratio is not identical for each configuration. Described below is the overall pressure ratio for each configuration:

For configuration I, the overall pressure ratio is $(p_{t,\infty}/p_e)_1$, where the pressure p_e is determined after model injection into a supersonic flow which was established at a particular stagnation pressure $p_{t,\infty}$. The minimum value of this pressure ratio represents the necessary tunnel operating conditions to maintain supersonic flow after model injection.

For configurations II and III, the overall pressure ratio is $(p_{t,\infty}/p_e)_2$, where the static pressure p_e is determined with the model in place and just prior to flow initiation and $p_{t,\infty}$ is approximately the minimum stagnation pressure for which supersonic flow could be established in the test chamber. This ratio is defined in this manner because it represents a repeatable parameter, which is compatible with the normal operation mode of blowdown-type facilities. The minimum value of this ratio represents the minimum pressure ratio necessary for establishing supersonic flow in the test chamber.

For configuration IV, the overall pressure ratio is $(p_{t,\infty}/p_e)_3$, where the pressure p_e is determined with the model in place and just prior to flow initiation and with the annular injector(s) operating at a stagnation pressure of 0.689 MN/m^2 and $p_{t,\infty}$ is approximately the minimum stagnation pressure for which supersonic flow could be established in the test chamber. The minimum value of this ratio represents the minimum pressure ratio for establishing supersonic flow in the test chamber with the aid of annular injector(s).

The absolute minimum overall pressure ratio necessary for starting was not necessarily obtained because of facility limitations in setting the desired levels of stagnation pressure or vacuum sphere pressure for each test. Since a Mach number near 1.0 would be expected to exist at the end of the diffuser constant-area section at the minimum starting pressure ratio, the average (area-weighted) Mach number near the end of the diffuser constant-area section was computed from measurements of static and pitot pressure in order to provide an indication of the minimum starting pressure ratio; the corresponding pressure recovery was obtained.

A restart pressure ratio $(p_{t,\infty}/p_e)_{restart}$ was determined for configuration IV. This ratio is that necessary to reestablish supersonic flow in the test chamber after the tunnel flow has been forced to go subsonic by throttling with a downstream valve. The static pressure p_e used in the ratio was determined after the flow was reestablished. The procedure was to have the injector(s) operating at a stagnation pressure of

0.689 MN/m^2, establish a supersonic tunnel flow, throttle the diffuser flow through the use of a downstream valve until tunnel unstart occurred, and then decrease the throttling until supersonic tunnel flow was reestablished.

In order to find the effect of injector total pressure on the chamber static pressure, the total pressure of the annular injector(s) was varied after supersonic flow had been established. The minimum ratio of chamber static pressure to free-stream static pressure p_c/p_∞ was used to describe the operating performance of the various model-tunnel test-section configurations.

Temperature and pressures were obtained by recording the output of iron-constantan and chromel-alumel thermocouples, and diaphragm and variable-capacitance-type pressure transducers on a Beckman 210 high-speed analog to digital data recording system. The accuracy of the data is believed to be as follows:

Tunnel total pressure, MN/m^2	±0.008
Cell and nozzle static pressure, kN/m^2	±0.068
Model and shroud static pressure, kN/m^2	±0.206
Diffuser static pressure, kN/m^2	±0.206
Diffuser pitot pressure, kN/m^2	±0.412
Injector total pressure, MN/m^2	±0.006
Nozzle and injector stagnation temperature, K	±1.1

RESULTS AND DISCUSSION

Configuration I, Model Injection

As shown in figure 4, the free-jet length for configuration I was the minimum necessary to allow model injection. The object of these tests was to set tunnel operating conditions so that supersonic flow would be maintained when the model was injected into the already established stream. Before model injection, the overall pressure ratio $p_{t,\infty}/p_e$ was 225; after model injection the overall pressure ratio $\left(p_{t,\infty}/p_e\right)_1$ was 117 and the corresponding ratio of chamber pressure to free-stream static pressure was 2.77. Figure 10 shows the Mach number and pressure recovery profiles near the end of the diffuser constant-area section. The average (area-weighted) Mach number and pressure recovery were 1.7 and 0.047, respectively. This pressure recovery corresponds to 76 percent of the normal-shock value.

Since the diffuser exit Mach number is somewhat greater than 1.0, the minimum overall pressure ratio $\left(p_{t,\infty}/p_e\right)_1$ is probably somewhat lower than 117. Figure 11 presents a schlieren photograph of the flow after model injection. As can be seen from the schlieren photograph, the shock waves emanating from this overexpanded nozzle impinge

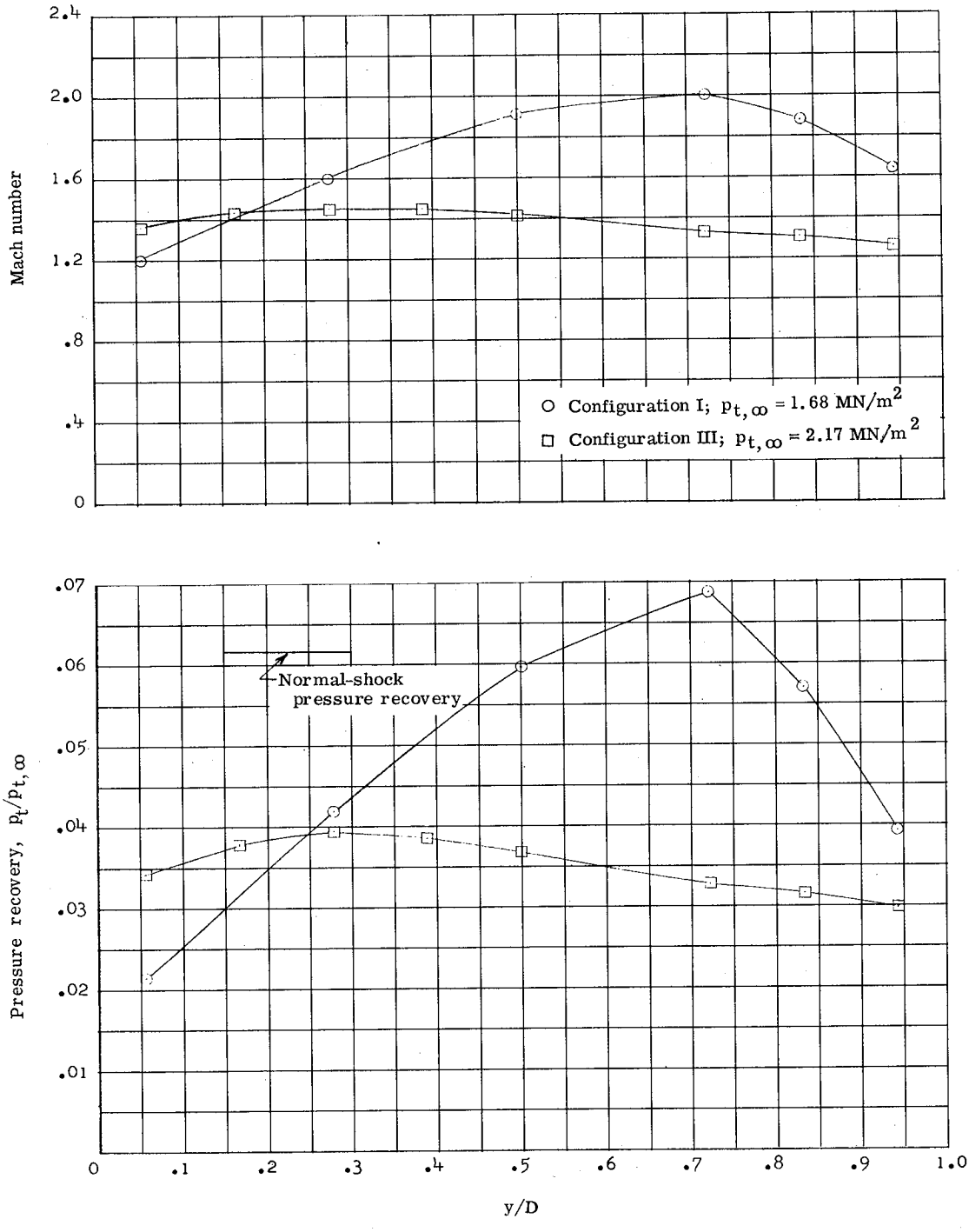

Figure 10.- Mach number and pressure recovery profiles near diffuser exit.

on the engine inlet spike. This condition, of course, would be an unacceptable flow condition for testing this model.

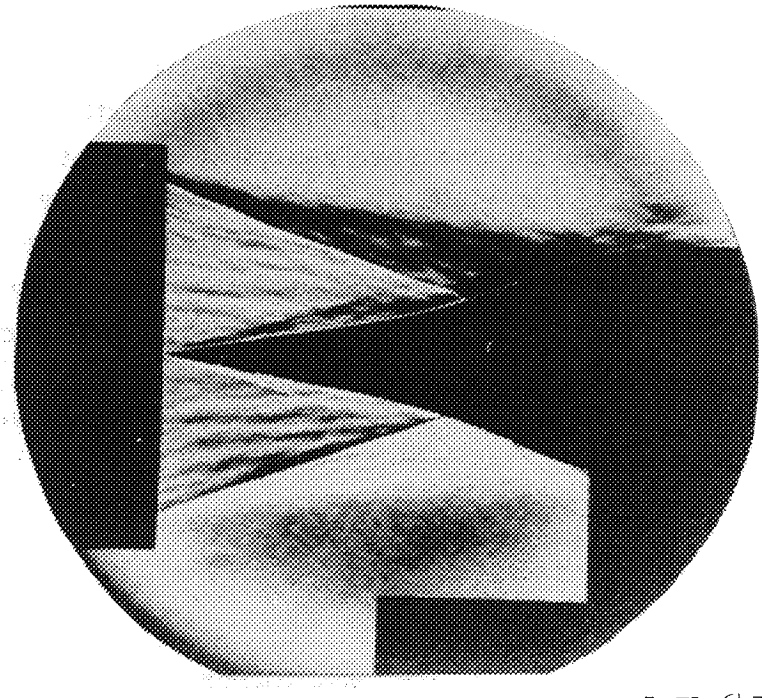

L-71-643

Figure 11.- Schlieren photograph. Configuration I; $p_{c,l}/p_\infty = 2.77$; $R_d = 3.6 \times 10^6$.

Configuration II, Diffuser Diameter

As can be seen in figure 5, the inlet spike was located 6.86 cm into the nozzle. This position was chosen for in-place starting in an attempt to keep the shocks from the nozzle wall from striking the inlet, to permit a small free-jet length, and to allow the flow field in the cowl lip area to be viewed by schlieren. Tests show that for $l/d = 1.44$, supersonic flow could not be established with either diffuser A or diffuser B. Overall pressure ratios $\left(p_{t,\infty}/p_e\right)_2$ as high as 2500 were investigated. A smaller free-jet length ($l/d = 1.22$) was provided by an extension to the scoop of diffuser A (see fig. 5); however, the extension did not improve the starting characteristics.

Configuration III, Shrouds

Since supersonic flow could not be established with either diffuser investigated with configuration II, a more efficient channeling of the flow around the model was considered to be beneficial to starting. The model shroud geometries shown in figure 6 efficiently channel the flow around the model and also allow pumping on the test chamber through the annular area between the shroud and the diffuser. Supersonic flow was established with shroud 1 and diffuser A (see fig. 6) with an overall pressure ratio $\left(p_{t,\infty}/p_e\right)_2$ of 92 and

the ratio p_c/p_∞ was 2.85. However, the area between the model mounting struts and the shroud had to be sealed because the leakage of the high internal shroud pressure into the chamber caused the tunnel to unstart after a short period of time. Mach number and pressure recovery profiles are shown in figure 10. The average (area-weighted) Mach number and pressure recovery was 1.3 and 0.035, respectively, this pressure recovery is 57 percent of the normal-shock value. Therefore, the starting pressure ratio of 92 is probably near the minimum starting pressure ratio that might be achieved with this configuration. Although shrouding the model allowed supersonic flow to be established, the chamber pressure remained high relative to the free-stream static pressure. Figure 12 presents a schlieren photograph of the flow and shows the relatively strong shock from the nozzle exit due to the high chamber pressure. The overall and chamber to free-stream static-pressure ratios did not vary with the annular area A_1 which was varied from 11.14 cm^2 to 27.51 cm^2. However, when the diffuser was moved forward to a position where no annular passage existed (diffuser diameter equal to the shroud outside diameter), supersonic flow could not be established even with an overall pressure ratio as high as 400.

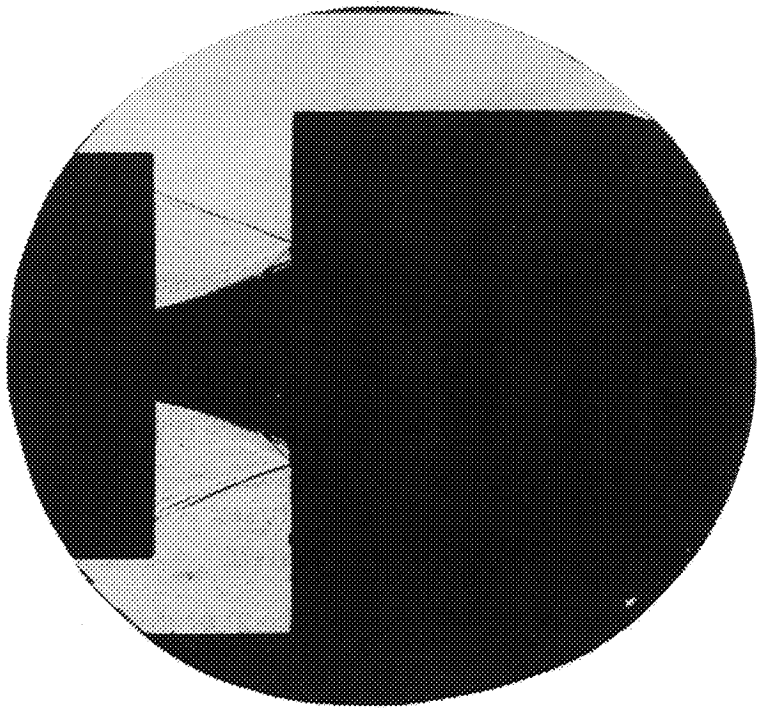

L-71-644

Figure 12.- Schlieren photograph. Configuration III; shroud 1; $p_c/p_\infty = 2.85$; $R_d = 4.1 \times 10^6$.

Supersonic flow could not be established with shroud 2, which is a smaller shroud configuration than shroud 1. The maximum overall pressure ratio investigated was 2500 and the annular area between the shroud and the diffuser was varied from no annular passage to the maximum area of 57.56 cm^2. The inability to establish supersonic flow with

this shroud configuration was probably due to the small area at the exit of the shroud. The flow through shroud 2 was compressed more than that for shroud 1 and resulted in a higher static pressure at the exit; this higher pressure would cause a decrease in the pumping effectiveness and therefore a higher test-chamber static pressure. This condition would be detrimental to starting.

Configuration IV, Annular Injectors and Shrouds

Because of the relatively high chamber pressure associated with configuration III (shroud 1), Mach 4 annular injectors at the tunnel nozzle exit (front injector) and the diffuser entrance (rear injector) were investigated in order to find the effect of mass injection on the chamber pressure and the starting characteristics. Two shroud configurations, shrouds 3 and 4 (see fig. 7), were investigated in conjunction with the annular injectors. In addition, the effect of angle of attack on tunnel starting was investigated.

Gas injection from the front or the combination of the front and rear injectors was required in order to establish supersonic flow with shroud 3. An overall pressure ratio $\left(p_{t,\infty}/p_e\right)_3$ of approximately 55 was sufficient to establish supersonic flow with the front injector operating and with the model at either $\alpha = 0^o$ or $\alpha = -4.5^o$. With the front injector operating at a total pressure of 0.689 MN/m^2 and the model at $\alpha = 0^o$, a restart pressure ratio $\left(p_{t,\infty}/p_e\right)_{restart}$ of 38 was obtained. At restart, the average (area-weighted) Mach number and pressure recovery near the end of the diffuser constant-area section ratio were 0.98 and 0.049, respectively. Therefore, the minimum overall pressure ratio for which supersonic flow could be established with the front injector operating and model at $\alpha = 0^o$ is estimated to be approximately 38. The tunnel could not be started with only the rear injector operating prior to the start of the main tunnel flow. The Mach number and pressure recovery distribution near the end of the diffuser constant-area section for the cases with mass injection from the front injector and with mass injection from the front and rear injectors are presented in figure 13. The ratio of chamber pressure free-stream static pressure and the total mass through the tunnel are equal for both cases. Figure 13 shows that the effect of the rear injector is to decrease the Mach number and pressure recovery, and this condition indicates a decrease in the performance of the system. Therefore, from the standpoint of Mach number and pressure recovery, the operation of the rear injector with shroud 3 appears to be detrimental to the system operation.

Figure 14(a) presents the effect of the injector stagnation pressure on the chamber pressure for shroud 3. For the case where injection was from the front and rear, the stagnation pressure of the front injector was used in the figure. The minimum chamber pressure with shroud 3 was 1.9 times the free-stream value, and the chamber pressure was not significantly affected by injector stagnation pressure. Figure 14(a) also shows

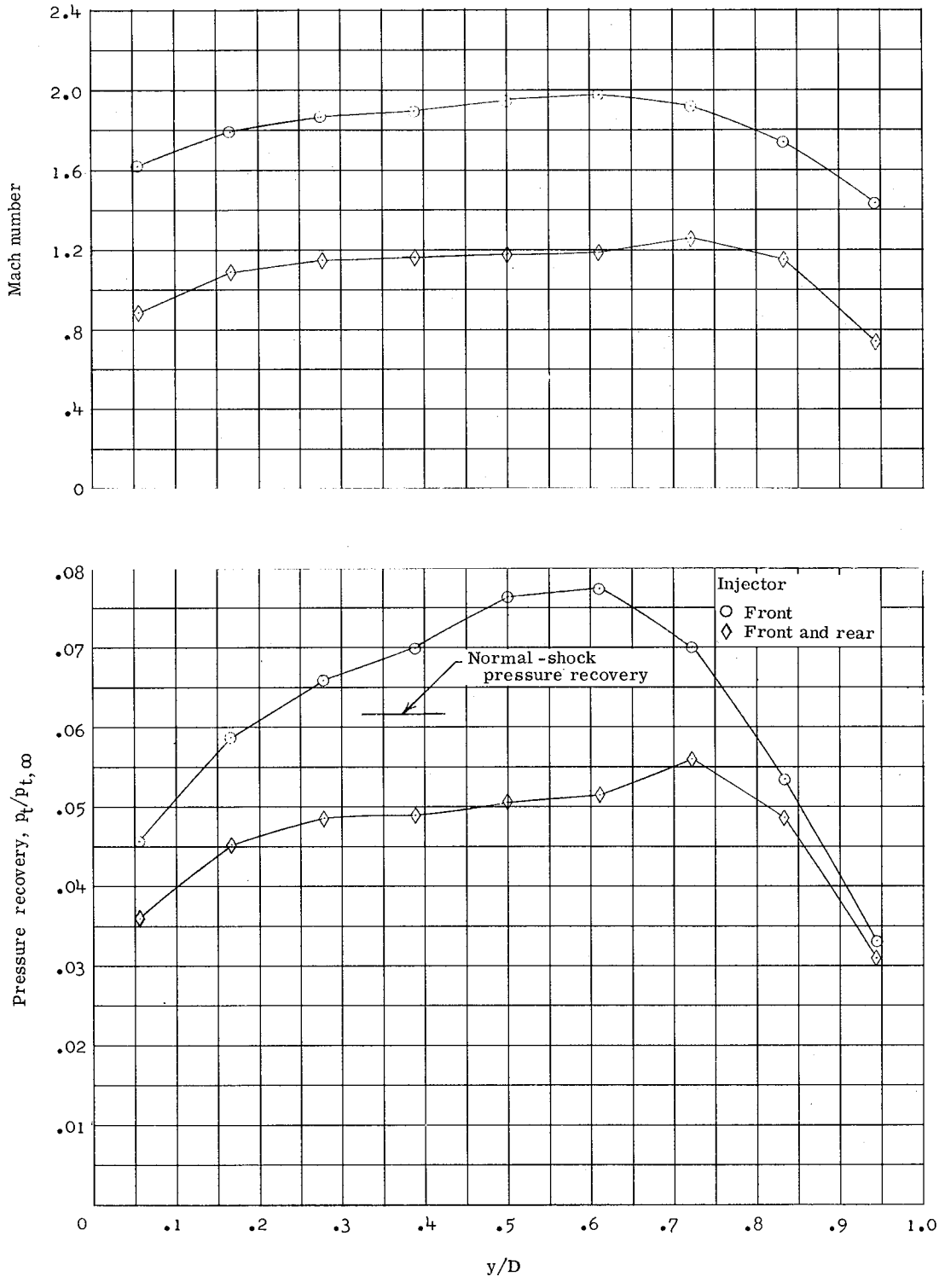

Figure 13.- Mach number and pressure recovery profiles near diffuser exit. Configuration IV; shroud 3; $p_{t,\infty}$ = 1.38 MN/m^2.

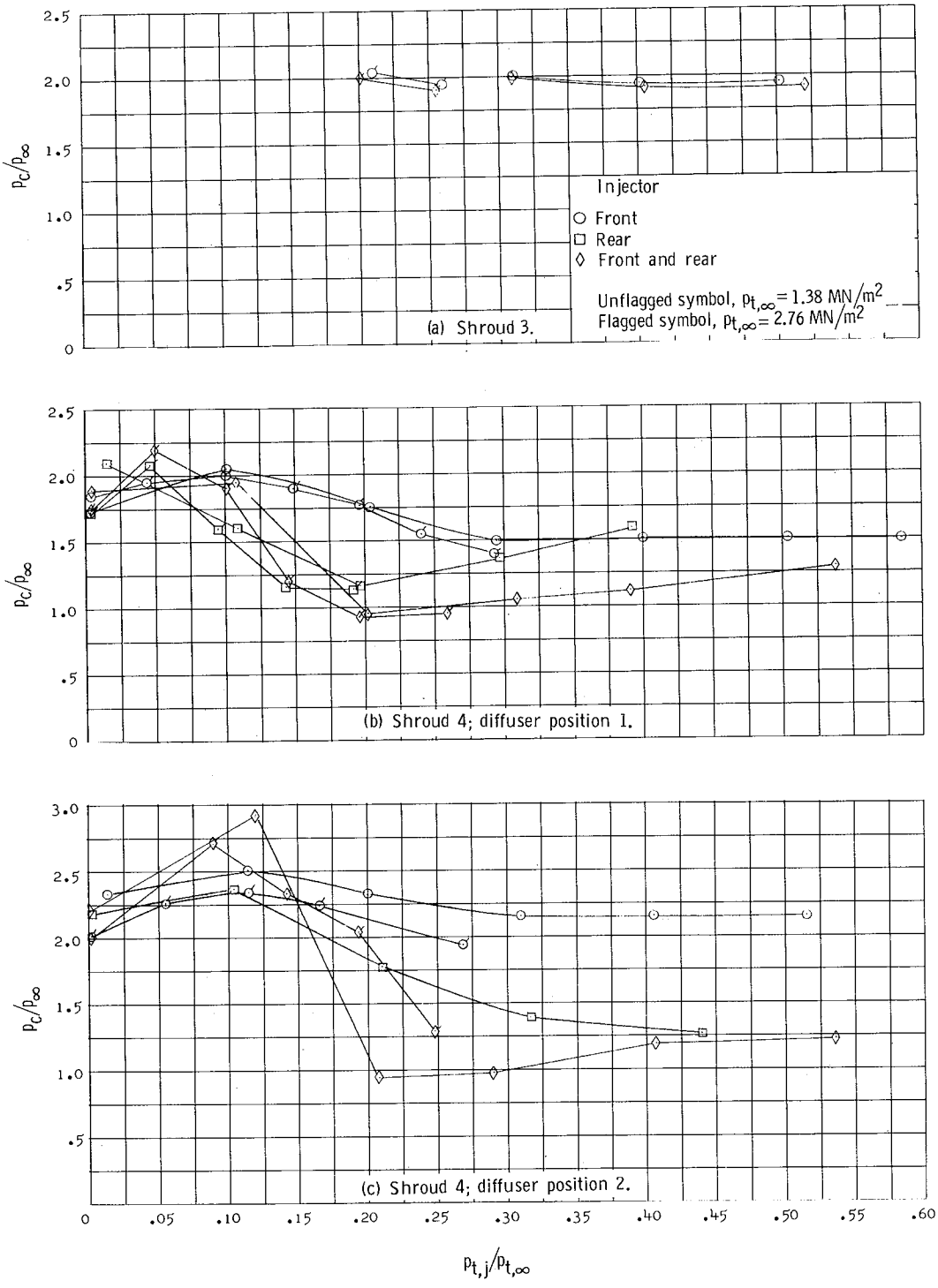

Figure 14.- Effect of injector pressure on chamber pressure. Configuration IV.

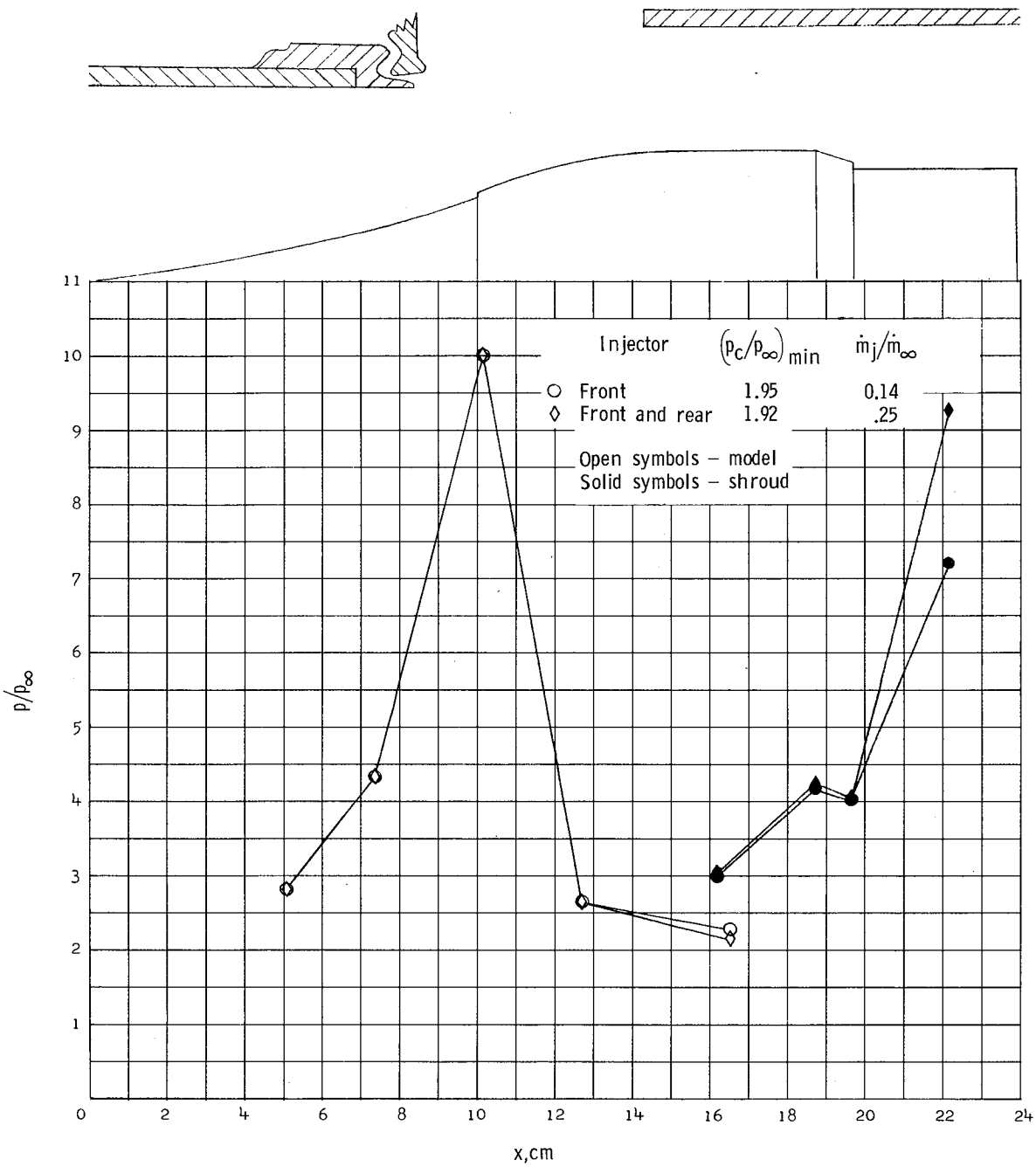

(a) Configuration IV; shroud 3; $p_{t,\infty}$ = 1.38 MN/m^2.

Figure 15.- Model and shroud static pressure.

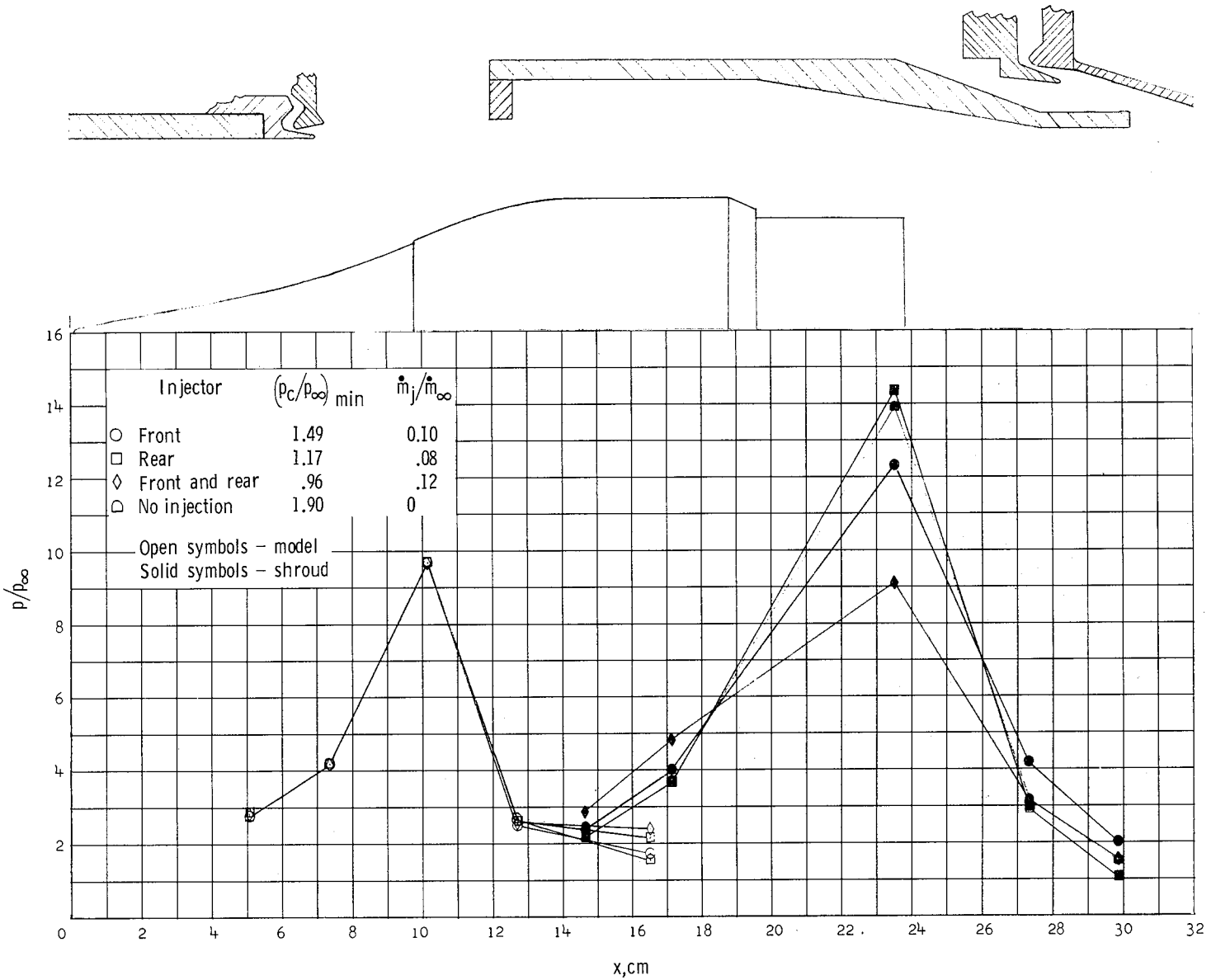

(b) Configuration IV; shroud 4; diffuser position 1; $p_{t,\infty} = 1.38$ MN/m^2.

Figure 15.- Concluded.

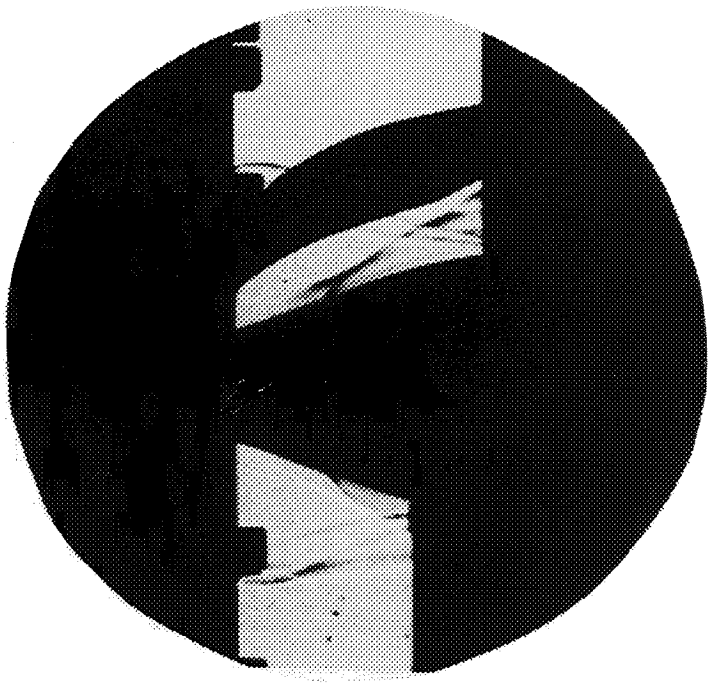

(a) Shroud 3; $p_c/p_\infty = 1.9$; $R_d = 3.0 \times 10^6$.

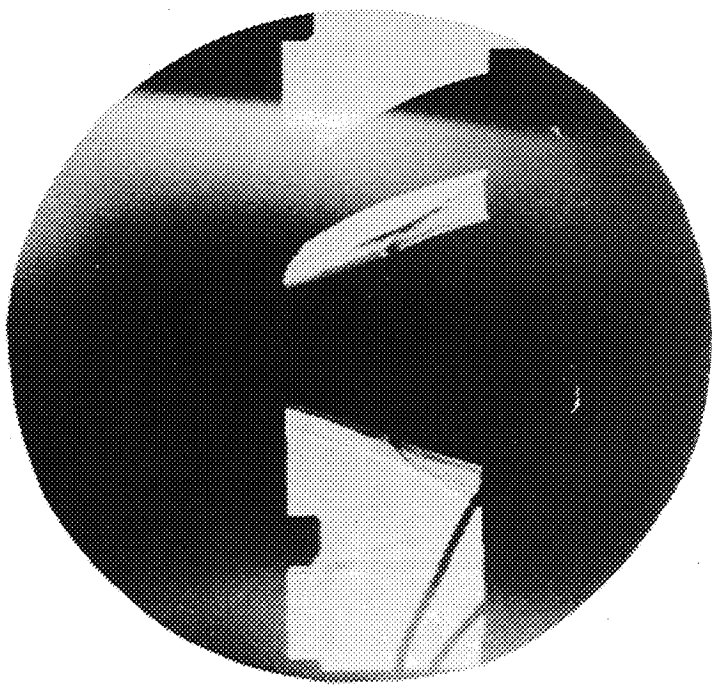

L-71-645

(b) Shroud 4; $p_c/p_\infty = 1.0$; $R_d = 3.0 \times 10^6$.

Figure 16.- Schlieren photographs. Configuration IV.

that the combination of front and rear injection did not lower the chamber pressure from the value attainable with injection from only the front injector. Therefore, with shroud 3, the rear injector does not appear to serve any useful purpose. With shroud 3, supersonic flow could not be maintained (1) for values of $p_{t,j}/p_{t,\infty}$ lower than 0.31 with $p_{t,\infty}$ equal to 1.38 MN/m^2, and (2) for values of $p_{t,j}/p_{t,\infty}$ lower than 0.20 with $p_{t,\infty}$ equal to 2.76 MN/m^2. The model and the internal shroud 3 static-pressure distribution are presented in figure 15(a). The pressure distributions correspond to the minimum values of p_c/p_∞; these values as well as the mass flow ratio $\dot{m}_j/\dot{m}_\infty$ that was necessary to produce the minimum chamber pressure are noted in the figure. A schlieren photograph of the flow is shown in figure 16(a).

Tunnel starting characteristics were investigated primarily with shroud 4 at diffuser position 1; however, the limited data obtained at diffuser position 2 shows similar starting characteristics. Supersonic flow could be established with shroud 4, $\alpha = 0^\circ$, and no gas injection with an overall pressure ratio of 47; only slightly lower overall pressure ratios were achieved with mass injection from the front, rear, or front and rear injectors prior to the start of the tunnel flow. The tunnel could also be started with shroud 4, $\alpha = -4.5^\circ$, and both injectors operating prior to the start of the main flow with an overall pressure ratio $(p_{t,\infty}/p_e)_3$ of 50. The starting characteristics with the model at $\alpha = -4.5^\circ$ and no mass injection were not investigated. With the front injector operating at 0.689 MN/m^2, a restart pressure ratio $(p_{t,\infty}/p_e)_{restart}$ of 35 was obtained. At restart the average (area-weighted) Mach number and pressure recovery at the end of the diffuser constant-area section were 1.01 and 0.051, respectively. Therefore, the minimum overall pressure ratio for which supersonic flow could be established with the model at $\alpha = 0^\circ$ and the front injector operating is considered to be approximately 35.

The data presented in figure 14 for shroud 4 show that chamber pressure is strongly dependent upon injector stagnation pressure, that chamber to free-stream static-pressure ratios of 1 can be obtained with mass injection from both front and rear injectors, and that diffuser position 1 generally results in lower chamber static-pressure ratios. An important feature of shroud 4 is that with mass injection from the front and rear injectors, the shock from the nozzle exit can be eliminated since the chamber static pressure can be matched with the free-stream static pressure. A schlieren photograph of the flow field with shroud 4 and $p_c/p_\infty = 1.0$ is shown in figure 16(b). Since lower chamber pressures were obtained with the rear injector than with the front injector and the combination of the front and rear injectors produced even lower chamber pressures, the rear injector in conjunction with shroud 4 was beneficial to the system operation. The flow from the front injector is underexpanded for $p_{t,j}/p_{t,\infty}$ greater than 0.308. Figures 14(b) and 14(c) indicate that when mass injection is only from the front injector, the minimum chamber

pressure is obtained when the injected flow is underexpanded and that when mass injection was from both the front and the rear injectors, the minimum chamber pressure occurs with the front injector operating in an overexpanded condition. This condition is believed to result because the most efficient operation of the rear injector occurred at an injector stagnation pressure which corresponded to the condition for which the front injector was operating overexpanded. However, since the pressure supply was common to both injectors, this assumption could not be verified.

The model and shroud 4 internal static-pressure distributions are presented in figure 15(b) for the minimum ratios of chamber to nozzle static pressure obtained with each mode of injection. The pressure distributions for diffuser position 2 showed the same trends as those shown for diffuser position 1. From the limited amount of pressure data presented in figure 15, the model and shroud static pressure distributions, with the exception of the peak shroud pressures, appear not to be significantly affected by the mode of mass injection.

With basic test conditions unchanged, the chamber pressure increased by a factor of 1.5 when the ring in shroud 4 was removed. Therefore, a ring identical to the one used in shroud 4 was installed in shroud 3 in order to determine whether addition of the ring would allow supersonic flow to be established without the use of the injectors. These tests indicated that even with the use of the injectors, supersonic flow could not be established with this configuration. Since shroud 3 did not extend as far forward as shroud 4, the flow from the nozzle is believed to have impinged on the ring and spilled into the chamber instead of entering the shroud. The ring was also tested in a position where the leading edge of the ring extended ahead of the shroud by 0.508 cm. Supersonic flow could be established with this configuration; however, no improvement in the starting characteristics from the original shroud 3 configuration were noted. That is, the ratio of chamber pressure to static pressure remained the same as that with no ring and the injectors were still required in order to establish and maintain supersonic flow. The good performance of shroud 4 is apparently because of the annular area for pumping on the test chamber and/or the fact that shroud 4 extended to the leading edge of the model mounting struts; thus, the high pressure flow in this region was channeled into the shroud.

In summary, the minimum starting pressure ratios were similar for shrouds 3 and 4. With shroud 3, mass injection at the nozzle exit was required for starting and maintaining the started condition, and the minimum chamber pressure was about twice the free-stream static pressure. In contrast, with shroud 4 no mass injection was required to establish supersonic flow and the ratio of chamber to free-stream static pressure was about 2, and with mass injection the chamber pressure could be matched to the free-stream static pressure. If use of only the front injector is considered to be desirable from a system standpoint, shroud 3 has the advantage of somewhat lower internal shroud

pressures than shroud 4 and, where a cooled shroud would be required, the construction of shroud 3 would be simpler than that of shroud 4.

CONCLUDING REMARKS

An experimental investigation has been conducted to develop simple expedients to achieve in-place tunnel starting with the characteristically high blockages associated with the testing of maximum size airbreathing engines in a relatively small tunnel. The model geometry investigated was that of the aerothermodynamic integration model of the hypersonic research engine. The cross-sectional area of this model was approximately 50 percent of the nozzle exit area. The investigation was conducted at Mach 5 at Langley Research Center in a test chamber which was modified to provide a 1/10-scale model of the Lewis free-jet hypersonic-propulsion research facility.

Supersonic flow could be maintained by injecting the model into an already established stream for the case where the free-jet length was 2.16 times the nozzle exit diameter, slightly greater than the engine length. The overall pressure ratio, the ratio of tunnel stagnation pressure $p_{t,\infty}$ to the static pressure near the end of the diffuser constant-area section p_e was 225 before model injection and 117 after model injection; the ratio of chamber pressure to free-stream static pressure was 2.77 after model injection. With the model fixed in the test position, and a free-jet length of 1.44 nozzle exit diameters, supersonic flow could not be established with overall pressure ratios of 2500.

The addition of a model shroud, which was designed to provide an annular passage between the conical entrance to the wind-tunnel diffuser and the external surface of the shroud, allowed supersonic tunnel flow to be established with the model in place and a free-jet length of 0.375 nozzle exit diameters. An overall pressure ratio of 92 was sufficient to establish supersonic tunnel flow with this shroud configuration and the ratio of chamber pressure to free-stream static pressure was 2.8. With a similar type of shroud, except for the addition of a ring at the shroud entrance, which was designed to restrict and reverse flow, and a free-jet length of 0.48 nozzle exit diameters, supersonic flow was established with a pressure ratio of 47. The ratio of chamber pressure to free-stream static pressure was 1.9.

When Mach 4 annular injectors at the nozzle exit and the diffuser entrance were used in conjunction with this type of shroud configuration, the starting characteristics were slightly improved and a ratio of test chamber pressure to free-stream static pressure of 1.0 was attained.

Mass injection from the nozzle exit injector was required in order to establish and maintain supersonic tunnel flow with a shroud configuration which did not have an annular passage between the conical entrance to the wind-tunnel diffuser and the external

surface of the shroud and for which the free-jet length was 0.69 nozzle exit diameters. With the annular injector at the nozzle exit operating, an overall pressure ratio of 50 was sufficient to establish supersonic flow with this shroud configuration. In addition, the operation of an injector at the diffuser entrance helped to achieve a tunnel start only when there was an annular passage between the conical entrance to the diffuser and the external surface of the shroud.

Langley Research Center,
National Aeronautics and Space Administration,
Hampton, Va., June 30, 1971.

REFERENCES

1. Anderson, D. E.: The Effect of Engine Size on Free-Jet Test Cell Performance. AEDC-TN-57-19 (ASTIA Doc. No. 144 313), U.S. Air Force, Nov. 1957.

2. Schueler, C. J.: An Investigation of the Model Blockage for Wind Tunnels at Mach Numbers 1.5 to 19.5. AEDC-TN-59-165, U.S. Air Force, Feb. 1960.

3. German, R. C.: Simulation of Supersonic Flow Over a Body of Revolution Using an Axisymmetric Jet Stretcher. AEDC TR 70-166, U.S. Air Force, Oct. 1970. (Available from DDC as AD 875 834.)

4. Smith, Forrest B., Jr.; Bauer, R. C.; and Barebo, R. L.: The Effect of a Jet Stretcher on the Flowfield About a 292 von Karman Body of Revolution at Mach Number 3.0. Paper No. 69-459, Amer. Inst. Aeronaut. Astronaut., June 1969.

5. McDevitt, John B.: A Study of Gas Injection in the Boundary Layer of a Hypersonic Wind Tunnel To Extend the Useful Operating Range. NASA TN D-2935, 1965.

NASA-Langley, 1971 — 11 L-7659